LINAC-LHC ep COLLIDER OPTIONS

F. Zimmermann, F. Bordry, H.-H. Braun, O.S. Brüning, H. Burkhardt, A. de Roeck, R. Garoby, T. Linnecar, K.-H. Mess, J. Osborne, L. Rinolfi, D. Schulte, R. Tomas, J. Tuckmantel, CERN, Switzerland; A. Eide, EPFL, Switzerland; F.J. Willeke, BNL, U.S.A.; S. Chattopadhyay, Cockcroft I., UK; B.J. Holzer, DESY, Germany; J. Dainton, M. Klein, Liverpool U., UK; A. Vivoli, LAL, France; S. Sultansoy, TOBB ETU, Turkey; A.K. Ciftci, Ankara U., Turkey; H. Aksakal, Nigde U., Turkey

Abstract

We describe various parameter scenarios for a linac-ring ep collider based on LHC and an independent electron linac. Luminosities between 10^{31} and 10^{33} cm^{-2}s^{-1} can be achieved with a s.c. linac, operated either pulsed or in cw mode with optional recirculation, at a total electric wall-plug power of order 20 MW. Higher luminosities of several 10^{33} cm^{-2}s^{-1} can be reached by investing more electric power or by energy recovery. Finally, merits of a linac-ring ep collider are discussed.

SCENARIOS

Colliding the LHC 7-TeV protons with a 25–140 GeV e$^{\pm}$ beam would both extend the discovery reach of the LHC, and enable precision physics with LHC data [1, 2]. e^{+}p collisions are desirable in addition to e^{-}p. One way to realize such ep collider is by installing a new lepton ring in the LHC tunnel, implying a new lepton injector too [3, 4]. The THERA study [5] inspired looks at an alternative LHC-based "QCD Explorer" colliding LHC protons with electrons delivered by a linac [6].

Possible linac-ring scenarios include a n.c. linac, a pulsed s.c. linac, and a cw s.c. linac with or without energy recovery in various configurations, as shown in Fig. 1.

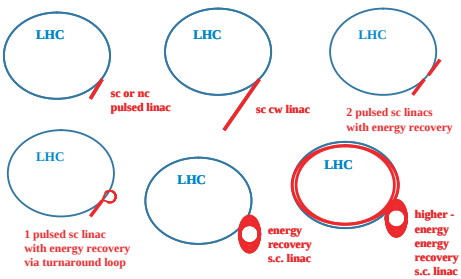

Figure 1: Scenarios for the linac-ring ep collider.

A s.c. linac can accelerate long trains of bunches with 25 or 50 ns spacing, matching the LHC fill pattern. Therefore, its luminosity in collisions with the LHC can be much higher than for a short-pulse low-charge and less efficient n.c. linac. The s.c. linac may have an rf frequency around 1.3 GHz, similar to ILC, or near 700 MHz, as for the CERN SPL. The bunch spacing is roughly 1/10 of the ILC's, at reduced charge per bunch. PLACET [7] simulations suggest that even with the ILC bunch charge of 2×10^{10} e^{-} the beam can be stabilized by a 0.1% detuning of the linac cavities. Energy recovery may be realized via a second linac pointing at the first one, in which the beam from the latter is decelerated [8]. More conventional energy recovery is possible by means of a recirculating linac, e.g. similar to ELFE [9], or with a turnaround loop as proposed for a future X-ray FEL [10]. Possible layouts are sketched in Fig. 2. For highest beam energy, the ERL with its recirculating arcs could be installed in the LHC tunnel itself, blurring the distinction between ring-ring and linac-ring LHeC options [11].

Table 1: Proton beam scenarios

	$N_{b,p}$	$T_{\rm sep}$	$\epsilon_p\gamma_p$	β_p^*
LHC	1.7×10^{11}	25 ns	3.75 μm	0.25 m
LHC*	5×10^{11}	50 ns	3.75 μm	0.10 m

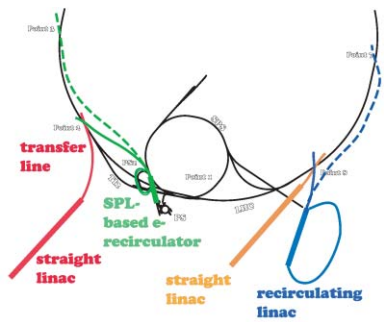

Figure 2: Example linac layouts on LHC site.

Two proton scenarios are listed in Table 1: (1) the nominal LHC beam combined with reduced proton interaction-point (IP) beta functions β_p^* of 0.25 m as foreseen for 2013, and (2) a higher brightness beam [corresponding to scenario "LPA" of [12]] available from an upgraded LHC injector chain, including a 5 GeV s.c. proton linac (SPL) and a 50-GeV synchrotron (PS2), by 2017. This second scenario also assumes $\beta_p^* = 0.1$ m, which may be possible by (1) focusing only one of the two proton beams, thereby relaxing aperture constraints; (2) dedicated ep runs, allowing for a chromatic correction twice as strong as for two low-β IPs; (3) reducing the free length l^* between the last proton quadrupole and the ep collision point; or (4) the hypothetical availability of (stronger) Nb_3Sn magnets.

ELECTRIC POWER

The cryogenics electric power for a s.c. linac is [13]

$$P_{\rm cr} = AE/g + BDEg\ , \qquad (1)$$

where the first and second terms describe the static and dynamic heat loads, respectively, making explicit their scaling with the rf duty factor D, the accelerating gradient in units

of eV/m g, and the energy gain over the length of the linac E. Inserting the parameters of the ILC and XFEL designs, we infer the values of the two coefficients A and B at 1.3 GHz [13]: $A \approx 350$ W/m and $B \approx 10^{-10}$ Wm/(eV)^2. A lower frequency of 700 MHz is likely to require less cryopower (up to 2 times less from BCS theory); the true difference depends on the residual resistance of the cavity Niobium, and other details. Figure 3 shows the cryogenic electric power for a 70 GeV beam as a function of accelerating gradient at $D = 1$ (cw mode) with and without a 4-pass recirculation, and at $D = 0.0075$ (pulsed mode).

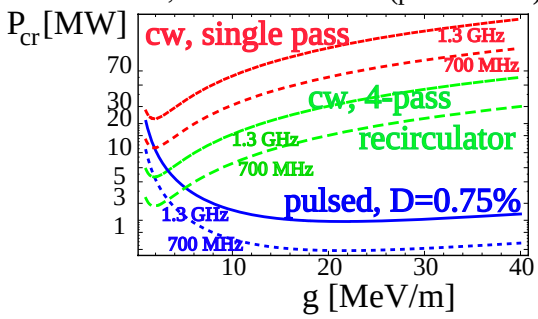

Figure 3: Cryogenics el. power vs. accelerating gradient.

The active length of the XFEL and ILC linacs is about 60% of the total. With a cavity gradient of 30 MV/m, the full length of a 60-GeV linac, without recirculation, would then be 3.3 km, and with 10 MV/m gradient it would be 10 km. The $\beta = 1$ section of the CERN SPL will be up to about 400 (or 256) m long and accelerate a beam by a maximum of 4.4 (or 2.9) GeV. With a 4-pass recirculation through this part of the SPL, an electron energy close to 20 GeV might be reached.

The rf electric power for a given beam power is $P_{\rm rf} = P_{\rm beam}/(\eta_{\rm rf\to beam}\eta_{\rm wp\to rf})(1-\eta_{\rm ER})$. From the XFEL and ILC designs, we infer a wall-plug power to rf efficiency $\eta_{\rm wp\to rf}$ of 50% for s.c. linacs. In cw modes of operation the rf to beam power conversion efficiency $\eta_{\rm rf\to beam}$ is taken to be 100%. In pulsed operation mode, additional rf energy is needed to pre-fill the accelerating structures, and the efficiency can be estimated from a reference design (subindex 'ref'; here the ILC) via $\eta_{\rm rf\to beam} \approx T_b/(T_b + (T_{\rm rf,ref} - T_{b,\rm ref})I_{\rm ref}/I)$ with T_b the beam pulse length, $T_{\rm rf}$ the rf pulse length, and I the beam current in the pulse. When we consider energy recovery options, the energy recovery efficiency factor is taken to be $\eta_{\rm ER} \approx 0.95$. In all other cases $\eta_{\rm ER}$ is set to zero.

LUMINOSITY

The electron beam size is assumed to be matched to the size of the protons, $\sigma_p^* = \sigma_e^*$, as a smaller electron beam could have adverse effects on the proton beam lifetime. Round-beam collisions are considered, since the linac beam generated by an e$^-$ gun is naturally round as are the LHC protons, and round beams maximize the luminosity for constant beam-beam tune shift. The luminosity formula then becomes

$$L = \frac{1}{4\pi e}\frac{N_{b,p}}{\epsilon_p}\frac{1}{\beta_p^*} I_e \; H_{\rm hg}\left(\frac{\beta_e^*}{\sigma_{z,p}}, \frac{\epsilon_e}{\epsilon_p}\right) , \qquad (2)$$

where e denotes the electron charge, and the subindices p or e refer to protons or electrons. The luminosity (2) depends only on the p beam brightness $(N_{b,p}/\epsilon_p)$ with $N_{b,p}$ the number of protons per bunch and ϵ_p the geometric emittance, on β_p^*, on the electron beam current I_e, and on the hourglass factor $H_{\rm hg}$. The term $(N_{b,p}/\epsilon_p)$ is limited by space charge in the proton injector complex and by the pp beam-beam tune shift. The electron current I_e is constrained by the linac technology, by the available electrical power, and by linac beam dynamics. The proton IP beta function β_p^* is confined, on the proton side, by the IR layout, as well as by the chromatic correction scheme, and on the electron side by the reduction factor due to the hourglass effect, $H_{\rm hg}$, given by

$$H_{\rm hg}(x,r) = 2\sqrt{\pi}xre^{\frac{4x^2r^2}{1+r^2}}\,{\rm erfc}\left(\frac{2xr}{\sqrt{1+r^2}}\right) . \qquad (3)$$

Figure 4 shows the minimum β_p^* that can be achieved for reasonable values of $H_{\rm hg}$ as a function of the normalized emittance at 60 GeV, and also $H_{\rm hg}$ vs. β^* for typical emittance values. To set this into perspective, the normalized emittance $\gamma_e\epsilon_e$ of the DESY XFEL design is 1.4 μm, while the smallest normalized emittance in LEP at 60 GeV was about 2 mm, i.e. $\sim 1000\times$ larger. Figure 4 underlines the potential of a low emittance linac beam to take advantage of small proton beta functions.

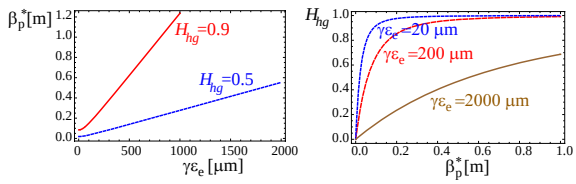

Figure 4: Proton IP beta function β_p^* vs. normalized electron emittance for two constant values of $H_{\rm hg}$ (left) and $H_{\rm hg}$ vs. β_p^* for three values of $\gamma_e\epsilon_e$ (right), assuming 60 GeV electron energy and $\sigma_{z,p} = 0.075$ m.

Figure 5 illustrates the luminosity reach vs. energy for various linac options considering a fixed wall plug power of 20 MW. One case with 100 MW was added to reveal the dependence on available power. The solid lines refer to the nominal LHC proton beam, the higher dashed curves to the 'LHC*' parameters of Table 1.

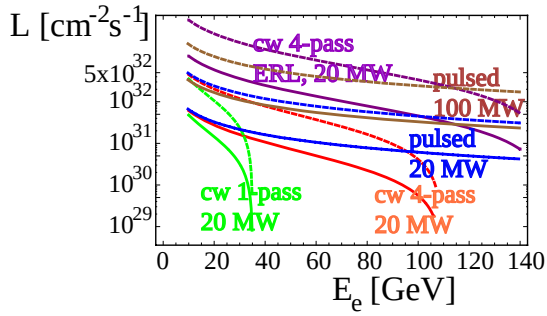

Figure 5: Luminosity vs. e$^-$ energy for cw & pulsed linac.

SOURCES

The e$^-$ beam can be produced from a polarized dc gun. Depending on the bunch charge, a normalized rms emit-

Table 2: Electron-beam parameters for various (s.c.) linac-ring LHeC scenarios. The β^* values are calculated for a normalized e- emittance of 20 μm. Parameters marked by asterisks refer to 'LHC*' of Table 1.

energy [GeV]	20	20	60	60	60	120
option	cw 4-pass	cw 4-p. ERL	cw 4-pass	cw 4-p. ERL	pulsed	pulsed
bunch population $N_{b,e}$ [10^9]	0.06, 0.12*	1.3, 2.6*	0.1, 0.2*	0.3, 0.6*	17, 34*	7, 14*
average current [μA]	400	8650	74	2050	820	340
beam power at IP [MW]	8.0	172	4.5	120	49	48
IP beta function [m]	0.25, 0.098*	0.25, 0.098*	0.74, 0.30*	0.74, 0.30*	0.74, 0.30*	1.72, 0.69*
luminosity [10^{31} cm^{-2}s^{-1}]	2.7, 20*	58, 430*	0.5, 3.7*	14, 100*	5.5, 41*	2.3, 17*
total electrical power [MW]	20	20	20	20	100	100

tance between 10 and 100 μm is expected after bunching and acceleration.

If the spent high-power e$^-$ beam is not passed through a turnaround loop to recover the e$^-$ energy [10], it can be used for e$^+$ production with subsequent interleaving of e$^-$ and e$^+$ bunches, or bunch trains, in the linac. This is possible since the colliding beams are round and the e$^-$ beam is only moderately disrupted by the collision (Fig. 6). The disruption angle $\theta_0 = D\sigma^*/\sigma_{z,p} = N_{b,p}r_e/(\gamma_e\sigma^*)$ [14] represents an upper bound on the divergence, and emittance, of the spent e$^-$ beam (right picture). The concept is sketched in Fig. 7, which also presents results of preliminary target and capture simulations, indicating a yield of up to 19 e$^+$ per e$^-$ for e$^+$ emittances $\gamma_e\epsilon_e$ of a few mm.

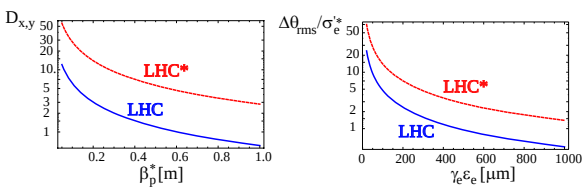

Figure 6: e$^-$ beam disruption parameter vs. β_p^*, and relative rms divergence increase in collision vs. initial $\gamma_e\epsilon_e$.

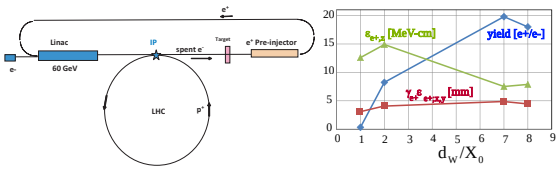

Figure 7: Schematic linac-ring collider with integrated positron production (left) and simulated e$^+$ yield for amorphous W target of varying thickness hit by a 60-GeV e$^-$ beam [$\gamma_e\epsilon_e = 20$ μm, $\sigma_{x,y,e} = 20$ μm, $\beta = 10$ m] (right).

MERITS

(1) Thanks to the small e^- emittance $\gamma_e\epsilon_e$ the luminosity can be increased for reduced β_p^*, and in addition the e$^-$ quadrupoles be positioned far from the collision point. The first elements are warm separation dipoles with 0.5–2 T field. A schematic IR layout is shown in Fig. 8. (2) The e&p beams can be collided head-on and no crab cavities are required, since the electrons are dumped and, with the assumed IR layout, residual parasitic collisions uncritical. (3) A staged construction is possible. A first stage could use the SPL as recirculator for alternating e$^-$/p operation, bringing the electrons to some 20 GeV, which would

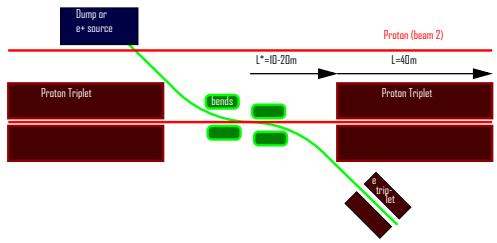

Figure 8: Schematic of linac-ring interaction region.

probe physics beyond HERA. Such SPL-based recirculator could later serve as injector for an electron ring or for an extended linac. The beam energy could be raised in steps by adding further linac segments. (4) As the linac is not affected by synchrotron radiation, there is no fundamental limit on the electron beam energy. (5) Implementation of energy recovery could ultimately gain another order of magnitude in luminosity. (6) Except for the collision point, the linac tunnel would be fully separate from the LHC, minimizing construction downtime. (7) The linac-ring collider would benefit from the planned proton infrastructure upgrades, i.e. linac4, SPL and PS2. (8) The e$^-$ beam can be 80% polarized. (9) Numerous important synergies with CLIC and ILC (beam dynamics, e+ production, tunnel, etc.) may well prepare the ground for a future linear collider. (10) Electron-ion collisions, as well as, via laser Compton backscattering, γ-proton and γ-nucleus collisions would also be possible.

REFERENCES

[1] S. Sultansoy, Eur. Phys. J. C33: S1064 (2004);
[2] J.B. Dainton et al, this conference.
[3] J.B. Dainton et al, JINST 1: P10001 (2006).
[4] H. Burkhardt et al, this conference.
[5] TESLA Design Report, DESY-01-011, Pt. 6, Ch. 2 (2001).
[6] D. Schulte, F. Zimmermann, Proc. EPAC'04 Lucerne, p. 632 (2004); H. Aksakal et al, Proc. PAC'05, p. 1207 (2005).
[7] D. Schulte, Proc. EPAC'00 Vienna, p. 1402 (2000).
[8] M. Tigner, Nuovo Cim. 37: 1228 (1965).
[9] K. Aulenbacher et al, ELFE at CERN, CERN-99-10 (1999).
[10] J. Sekutowicz et al, PRST-AB 8:010701 (2005).
[11] V. Litvinenko, CERN AB Forum 11 March 2008.
[12] F. Zimmermann, Proc. PAC'07, p. 714 (2007).
[13] A. Eide, Project Report, EPFL Lausanne (2008).
[14] P. Chen, K. Yokoya, PRD 38, 3, 987 (1988).